Leadership in Sustainable Infrastructure
Leadership en Infrastructures Durables

Vancouver, Canada
May 31 – June 3, 2017/ *Mai 31 – Juin 3, 2017*

OPTIMAL NEAREST NEIGHBOR CALCULATION FOR AUTOMATED RETRIEVAL OF CONSTRUCTION ELEMENTS FROM CLUTTERED POINT CLOUDS

Sharif, Mohammad-Mahdi[1, 7], Jeanclos, Nicolas[2], Kwiatek, Caroline[3], Nahangi, Mohammad[4], Haas, Carl[5] and West, Jeffrey[6]
[1] Ralph Haas Civil Infrastructure Sensing Laboratory, Department of Civil and Environmental Engineering, University of Waterloo, Canada
[2, 3] Ralph Haas Civil Infrastructure Sensing Laboratory, Department of Civil and Environmental Engineering, University of Waterloo, Canada
[4] Post-Doctoral Research Associate, University of Waterloo, Canada
[5, 6] Ralph Haas Civil Infrastructure Sensing laboratory, Department of Civil and Environmental Engineering, University of Waterloo, Canada
[7]mohammad-mahdi.sharif@uwaterloo.ca

Abstract

3D point cloud data can be used for visual and quantitative dimensional control of an object of interest but requires a robust post-processing algorithm to isolate the object being considered from the clutter in the point cloud. Finding an object in a scene is a crucial task that has been investigated extensively in literature. Once the object is found it must be isolated using a clutter removal methodology. One such methodology used the KNN algorithm. This paper presents a case study on finding the optimal threshold value of the K value in the KNN algorithm. Tests have been carried out on a cylindrical pipe spool assembly. Two criteria for measuring the success of clutter removal have been defined as: (1) Number of points erroneously remaining in the point cloud. (2) Number of points erroneously removed. These two criteria have been measured under different scenarios by changing the quality of the assembly, the number of points in the scene point cloud, and the number of points in the model point cloud. The contribution of this paper is providing a mathematical solution for selecting an optimal threshold value for the K value in the KNN algorithm to ensure that only excessive points are removed from the scene point cloud once the object of interest is identified.

1 Introduction

3D image acquisition tools are becoming more prevalent in the construction industry as they have become more affordable and as design information shifts from traditional 2D drawings to 3D BIM (Building Information Model) models. 3D scanners enable their users rapid access to accurate information regarding the geometric conditions on a job site or in a construction facility. Traditionally, laser scanners have been the most reliable and accurate source of 3D data (Bosche & Haas 2008). Photogrammetry and structured light scanners offer lower cost solutions but with compromised accuracy. (Golparvar-Fard et al. 2009). Increased competition, demand and innovation is pushing the development of all areas of 3D data acquisition and is resulting in higher quality technology being available at increasingly lower prices.

One area of substantial use of these tools is the development and implementation of scan vs. BIM framework for early detection of construction defects. Typically, 15% of construction rework is due to late detection of defective components (Burati et al. 1987). Late detection of defects can result in project schedule delays, cost overruns and cost propagation in projects with sensitive schedules. Consequently, early detection of defects in construction projects has become a prime concern for stakeholders. Geometric

non-compliance is a major source of defects in construction. Advancements in 3D image acquisition tools have enabled users to access to geometric data in real-time and made early detection of such deficiencies feasible (Brilakis et al. 2012). Comparing the design information to the as-built data provides an assessment of the fabrication quality and can be done by superimposing the 2 point clouds (3 by n matrices of geometric coordinates) to inspect the geometric compliance of the completed assembly.

One of the challenges with comparing a scan point cloud with a model point cloud is that the scan contains clutter points, which are points from the object's environment that get captured when acquiring the scan. To compare the 2 point clouds the object of interest must be isolated in the scan by removing the clutter points. To isolate the object of interest, the object must first be found within the point cloud before the clutter can be removed. To find the object, the Random Sample Consensus (RANSAC) algorithm proposed by (Papazov, Burschka 2010) was used. Once the scene point cloud has been superimposed onto the design point cloud, post-processing algorithms have to be employed to properly isolate the object of interest by removing the clutter. Automating the accurate extraction of objects of interest from spatial data is the fundamental enabler for further developments in automated spatial analysis. The goal when decluttering a point cloud is to isolate the points that correspond to the object of interest from a complete point cloud without removing points belonging to the object of interest. Figure 1 shows the process for isolating an object of interest from a scene point cloud.

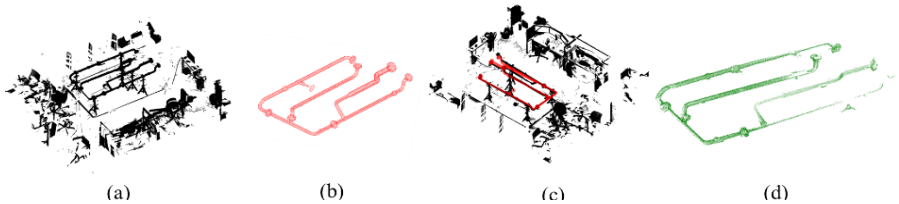

Figure 1. Abstract of the process from scan acquisition to object isolation. (a) Acquired scan of the scene including clutter points. (b) BIM model of the object of interest in point cloud format. (c) Model superimposed on the scan. (d) Resulting point cloud after applying clutter removal algorithm.

Classification methods have been investigated in literature and multiple algorithms have been developed by researchers. One such application of the algorithms is clutter removal, where classification methods facilitate the retrieval of objects from point clouds. These methods include graph-cut based method (Pan & Taubin 2016) and structure less nearest-neighbor techniques composed of K-nearest neighbors methods (Bhatia & Vandana 2010). Nearest neighbor search algorithms have been found to be the most effective (Bajramovic et al. 2006) for removing clutter. A variety of KNN searching algorithms are used in point cloud modeling (Zhao & Meng 2009) to calculate surface curvature (Li et al. 2014) in addition to noise and clutter removal.

KNN is acknowledged as a simple, robust and effective method for classification of points as belonging to either the object of interest or to the clutter. Nonetheless, KNN still faces two main shortcomings as a post-processing technique (Jiang et al. 2007): 1) The distance function used to measure the differences and similarities between the 2 point clouds is the standard Euclidean distance, and 2) the neighborhood size is artificially assigned as an input parameter K, biasing the algorithm by the arbitrary nature of the K value chosen. Since the accuracy of the algorithm is highly dependent on the K value, researchers have proposed several models for selecting this value. For example, Xie proposed a model named Selective Neighborhood Naive Bayes, also known as SNNB (Xie et al. 2002). The basic idea is that multiple K values are tested and the one with the highest estimated accuracy to classify the data is selected. As stated in (Guo et al. 2003), the simplest approach to selecting the K value in this model is to run the algorithm multiple times with different K values and to identify the K associated with the best trial.

To evaluate the success of the exclusion of clutter from the point cloud, the method presented in this paper uses two measures: 1) number of points erroneously remaining in the point cloud, 2) number of points erroneously removed from the point cloud. The main contribution of this work is the selection of an optimal K value depending on the number of points in the as-design point cloud and in the as-built point cloud. The

method was administered on cylindrical objects (pipe spools). The accuracy of the model was tested and found to have an R square value equal to 0.75.

The paper is organized as follows. In section 2, a survey of 3D imaging methods in construction and post-processing techniques for finding the object of interest in a point cloud is provided. In section 3, the methodology for the experiment conducted is described. In section 4, includes details of applying the proposed methodology. Discussion and future works has been discussed in section 5.

2 Research Background

Two main areas have been investigated: 1) the use of 3D-imaging in construction and 2) post-processing algorithms for removing clutter in point clouds. A focus was placed on K-Nearest Neighbor post-processing algorithms as this study utilized a KNN technique as the primary method for the clutter removal algorithm.

2.1 3D-imaging in construction

There are three main 3D image capturing technologies available: laser scanning, photogrammetry and structured light. Laser scanners typically use the time of flight of a light ray being sent and received by the sensor to capture the distance of a point on an object being investigated (Bosch et al. 2001). Photogrammetry uses multiple 2D images of the desired scene and utilizes a variety of available algorithms to reconstruct the scene point cloud. For more information on current methods for reconstructing point clouds using 2D images please refer to Remondino et al. 2015. Structured light sensors measure the three-dimensional shape of an object using projected infrared light patterns and a camera system (Furht & Ahson 2008). Structured light sensors are available in several commercialized 3D scanners. However, as shown in (Sharif et al. 2016), these technologies currently struggle to capture an object that exceeds two meter in the principal length.

Currently, ground-based laser scanners are the superior acquisition technology used as they can provide the highest accuracy and density point clouds. Bosche and Haas used laser scanners to develop a frame work for construction object recognition using the projection of the BIM model onto the relative position of the scanner (Bosche & Haas 2008). Turkan presented a framework for automatic project schedule updating based on the object recognition method previously developed by Bosche (Turkan et al. 2012). Nahangi developed a method for progress tracking using robotics analogy and forward kinematics with a focus on mechanical, electrical and piping components (Nahangi et al. 2015).

Coupling 3D design models with the acquisition of high quality 3D spatial data has made it possible to directly compare a completed industrial component with its design model. Akinci presented a method for comparing as-planned 3D design information (CAD model) with periodic imaging of critical construction components (Akinci et al. 2006). A great deal of research has gone into using 3D designs with 3D spatial data to evaluate pipe spool assemblies as they are critical for industrial construction projects including refineries and power plants. Pipe spool assemblies are typically prefabricated in shop and then sent to the site to be assembled which requires accurate fabrication and an incident-free transportation to the site. In 2003, the Construction Industry Institute reported that 13.3% of all fabricated pipe spools in the industrial sector required rework (CII, 2003). This has prompted researchers to investigate methods to better regulate the prefabrication to ensure that spools are being fabricated within tolerance. Nahangi developed an automated approach for monitoring and assessing fabricated pipe spools and structural systems using automated scan-to-BIM registration (Nahangi et al. 2015, Nahangi & Haas 2014). The method reliably detects the presence of dimensional non-compliance. Lee introduced a new method to extract critical points and centerlines in pipelines to reconstruct the model and compare it with BIM for progress tracking (Lee et al. 2012). These methods still leave room for improvement and further development to better assess the as-built conditions of pipe spools.

2.2 Post-processing algorithm: retrieval of object-of-interest

Manually removing clutter is a tedious task that requires automation to allow it to be part of a practical 3D imaging application in construction. Researchers have investigated and developed multiple frameworks using nearest neighbor (NN) methods for finding and recognizing objects of interest in point clouds

(Czerniawski et al. 2016). NN methods can be classified into two categories: 1) Structure Less NN techniques, which overcome the memory limitation issue, where the whole data sets are classified into training data and sample data points and distance is then calculated to find the nearest neighbor, and 2) Structure Based NN algorithms which reduce the computational complexity by structuring the data into different organisations such as Ball Tree (Liu et al. 2006), KD-Tree (Friedman et al. 1977) and NB-Tree (Kohavi 1996). In this study, a KD-Tree was used to structure the points of the point cloud in a 3D space. An Approximate Nearest Neighbor Search algorithm was then performed on the sorted data to extract the desired points from the point cloud. Jiang surveyed improved KNN search algorithms that either improve the distance function, the neighborhood size or the class probability estimation (Jiang et al. 2007). The attributes are weighted when calculating the distance and then the K value that best fits the data is determined.

The main contribution of the present paper is to develop and evaluate an effective process that facilitates the retrieval of an object from a point cloud scene. The method was applied to cylindrical objects, pipe spools, and presents a mathematical solution to determine the optimal K-value to retrieve an object of interest from a cluttered point cloud.

3 Methodology

The methodology for optimal object retrieval of cylindrical objects from point clouds and the flow of information between various components is illustrated in Figure 2. The objective of proposed method is to determine a mathematical solution to find the optimal threshold value in the decluttering process utilizing a KNN (K Nearest Neighbour) algorithm. KNN is performed to remove points in the scan point cloud that do not correspond to the model point cloud. For each point in the model, K points in the scan point cloud that are closest to that point will be selected and stored in a new point cloud or matrix. The goal is to store all the points from the scan that correspond to the model and remove all the points that are considered clutter. Increasing the threshold value (K) in the algorithm will increase the number of clutter points that are accepted as corresponding to the model (False Positive) and decreasing the K value will increase the number of points corresponding to model that are incorrectly deemed to be clutter (False Negative) (Figure 6).

Two criteria have been defined to determine how successfully desired points are extracted from the scan for each K value. The criteria are defined as follows:

[1] Void Rate (VR) = $\frac{\text{Number of points corresponding to model removed erroneously}}{\text{Number of points in the point cloud after applying KNN}}$

[2] Noise Rate (NR) = $\frac{\text{Number of clutter points accepted erroneously}}{\text{Number of points in the point cloud after applying KNN}}$

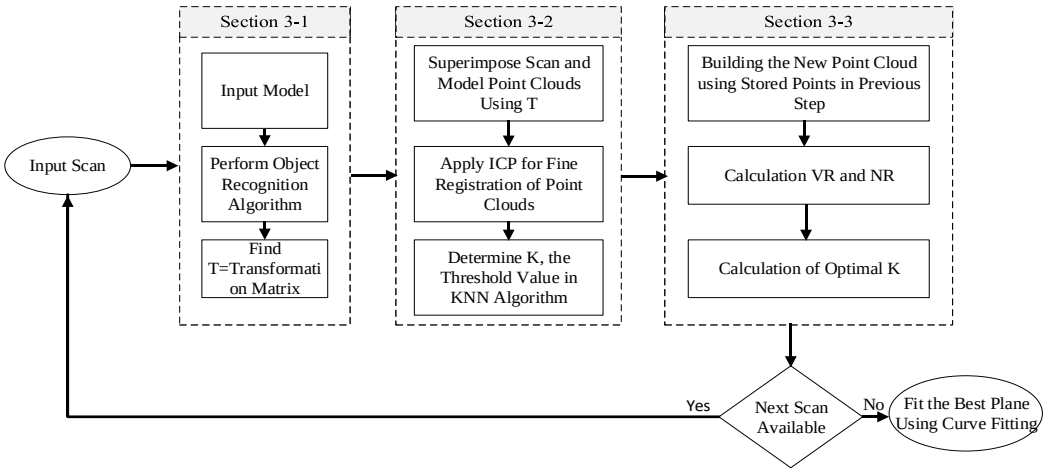

Figure 2. Research methodology and the flow of information between different components.

The optimal K value is one where both VR and NR are minimized. Assuming that minimizing both criteria is of equal importance, the optimal value will be determined by intersecting VR (Void Rate) and NR (Noise Rate) trend lines (Figure 6). Experiments were carried out on a pipe spool assembly at The Ralph Haas Infrastructure and Sensing Analysis laboratory at the University of Waterloo. The assembly measures approximately $2\text{m}\times1.5\text{m}$ consists of 4 individual pipe spools. (Figure 3)

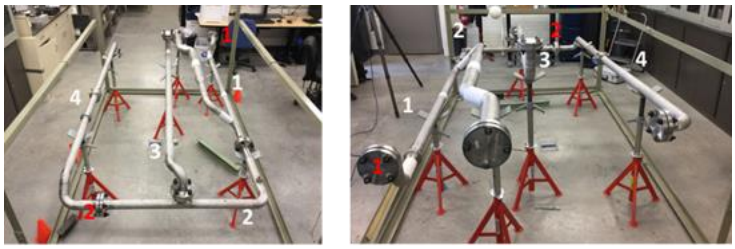

Figure 3. The test pipe spool assembly. Angular distortions to the assembly were induced at the flange numbers one and two, numbered in red. Branches are numbered in white for further reference in the article.

3.1 Finding the object of interest

A set of experiments was carried out on an industrial pipe spool to verify the proposed methodology for optimal clutter removal using a KNN algorithm on cluttered 3D point clouds. The object-of-interest, the pipe spool, is located in a laboratory environment and is surrounded by other unwanted objects that get scanned resulting in noisy point clouds. A FARO LS 840-HE laser scanner (with accuracy of ± 3*mm* at 25*m)* was used to acquire 3D point clouds.

Five different scenarios were generated using the pipe spools. Four scans were taken from different locations for each scenario. The four scans were taken to ensure that a complete representation of the assembly in each scenario was captured. The first scenario is the case were the assembly complies with the design. In second scenario a rotational error has been imposed on flange number 1. The third scenario has a rotational error imposed at flange number 1. In the final two scenarios, the assembly was disassembled into its component spools (Figure 4) and the component spools were each individually tested for optimal extraction. In the fourth scenario all the individual spools comply with their designs and in the fifth scenario deviations have been imposed on branches one and four. A total of 12 scene point clouds were acquired.

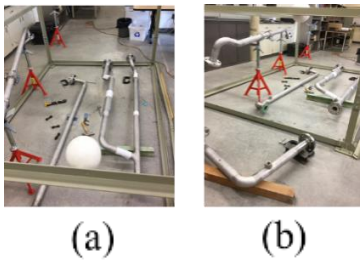

Figure 4. Disassembled spools for scenarios four and five. (a) All spools are compliant to the design. (b) Branch numbers one and four have been distorted.

Once scanning is completed the object must be found in the scans. This study utilized the algorithm provided by (Papazov, Burschka 2010) to find the object of interest. This algorithm requires two inputs. The first input is the BIM (as-designed) model in Stereo Lithography (STL) format. The second input is the scene or the as-built point cloud. Once the two inputs are loaded into the object recognition algorithm, a transformation matrix is computed and outputted. The transformation matrix is a 4×4 matrix which consists of a 3×3 matrix describing a 3D rotation of the point cloud and 3×1 vector describing the translation. From the twelve acquired scenes, ten had the object of interest detected by the object recognition algorithm.

3.2 Point Cloud Isolation

In order to ensure that all the surfaces of the object of interest (pipe spools) were captured, scans were taken from four perspectives. These four scans were then merged into a single point cloud. The operation of merging point clouds of the same scene, taken from different angles, is referred to as registration. To register a point cloud, three corresponding points must be identified and selected in each scan. White spheres (shown in Figure 3) were placed in the scene to be used as the corresponding points between scans for registration. “Faro Scene,” a commercially available software was used to merge the point clouds together. Once the scans were registered, the resulting point cloud was down sampled from its initial two million points to approximately two hundred thousand points. The initial point cloud was too dense for the purpose of this study and down sampling allowed the computation time to be reduced for the algorithm. Down sampling populates a new point cloud by sampling points from the original point cloud and was done according to Poisson-disk distribution which resulted in point cloud where the points were equally distributed across all surfaces. In other words, an equal number of points would be found for any two arbitrarily chosen surfaces of equal area. For more information on the down sampling algorithm please refer to (Corsini, Cignoni et al. 2012).

Given the two point clouds and the transformation matrix the extraction of the object of interest was calculated (see Algorithm 1). A third point cloud was calculated using stored points from the scene point cloud that have been determined to correspond to the model point cloud. The filtering process was performed using a KNN algorithm. This study includes an iterative step where the K value changes to examine its effect on the success of object extraction. The processes in this section are summarized below in Algorithm 1.

3.3 Calculation of Void Rate and Noise Rate

After down sampling and performing Algorithm 1, the success of Algorithm 1 was measured by performing Algorithm 2, described below. The success of object extraction was measured with two defined criteria. As explained in Section 3.1, Void Rate and Noise Rate are the two parameters for measuring the accuracy of the extraction. The accuracy was changed by changing the K value. Figure 5 shows an example of a false positive and false negative.

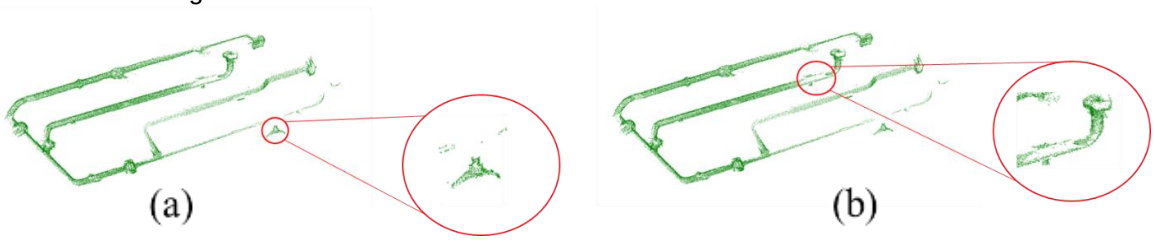

Figure 5. Challenges of removing clutter points without removing points on the object of interest. (a) Example of remaining clutter points after clutter removal for K equal to 8. (b) Example of removed points from the object of interest for the same K value.

3.4 Best Fit and Optimization

After performing Algorithm 2, a set of VR and NR values was calculated where each member of the set was calculated based on a distinct K value. To find the optimal K value for each scan, NR and VR values were graphed with respect to their corresponding K value as shown in Figure 6. Once tabulated, trend lines were fitted to each data set. The optimal K value for each scan was then calculated based on the intersection of the trend lines. The intersection point was found by solving the system of equations created by the two trend lines. This process was repeated for all of the scans acquired. MATLAB’s curve fitting tool was used to fit the data set of optimal K values and the size of the corresponding model and scan point clouds to a mathematical model. The results of this section are discussed in Section 4. Algorithm 3, used to fit the mathematical model, is described below.

4 Results

Applying Algorithms 1 and 2, as defined in Section 3, will generate VR and NR values for each K value used for each scene considered.

Table 1 provides a summary of the results obtained by applying the algorithms on scene one (compliant spool assembly).

The headings used in the table are defined as follows:

M: number of points in model point cloud, S: number of points in scan point cloud, K: threshold value used in KNN search algorithm, N: number of points in isolated point cloud, m: number of points after manually removing noise in initial scan point cloud, n: number of points in the isolated point cloud that correspond to the object of interest, q: number of points in the isolated point cloud.

Table 1. VR and NR values computed using different K values for scene 1

M	S	K	N	m-q	n-q	q	VR	NR
12061	81272	1	3546	33	2648	6161	0.42	0.005
12061	81272	7	5447	437	1151	6161	0.18	0.07
12061	81272	10	5668	481	974	6161	0.158	0.078
12061	81272	50	6882	776	55	6161	0.009	0.125
12061	81272	110	7464	1307	4	6161	0.006	0.2121
12061	81272	285	7935	1798	24	6161	0.003	0.29

Figure 6 shows the curves that were fit to the data summarized in

Table 1. VR and NR must be minimized to find the optimal K value for each scan. To do so, a trend line was fitted to both the VR and NR data sets. The optimal K value was calculated as the solution to the system of equations created by the VR and NR trend lines. Figure 6 graphically depicts the calculation of the optimal K value for scan number one.

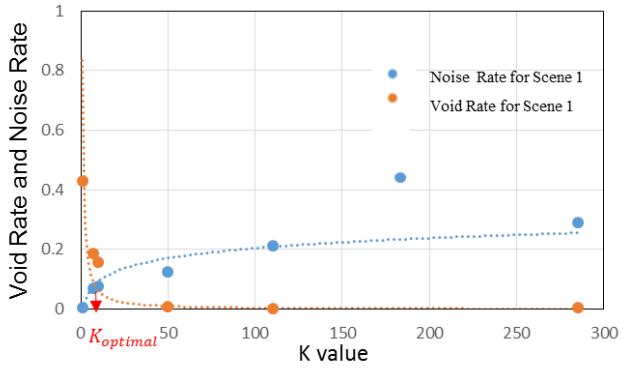

Figure 6. Calculation of optimal K at the intersection of VR and NR trend lines

For each scan, a logarithmic equation was used to fit a line to the void rate (VR) data points while a power equation was used to fit a line to the noise rate (NR) data points. Equations [4] and [5] below illustrate the general formats of equations that were used to calculate the trend lines that best fit the data points.

[4] $Y = a \ln(x) + b$ and R_1^2

[5] $Y = á\, x^{b́}$ and R_2^2

In equation [4], $R_1{}^2$ denotes the root mean square values between the observed data points and the corresponding VR values predicted by the trend line. Similarly, $R_2{}^2$ denotes the root mean square values between the observed data points and the corresponding NR values predicted by the trend lines. Solving the system of equations defined by equations 4 and 5 provides the optimal K value for each scan.

Table 2. Parameter values for fitted lines and subsequent optimal K calculation.

Scene No.	a	b	$\acute{a}$	$\acute{b}$	$R_1{}^2$	$R_2{}^2$	$K_{optimal}$
1	0.0487	-0.0195	0.832	-1.12	0.92	0.81	11
2	0.036	-0.035	0.2478	-0.495	0.87	0.83	17
3	0.052	-0.0417	0.0458	-0.273	0.96	0.46	6
4	0.196	-0.2294	0.0965	-0.122	0.66	0.45	7
5	0.2938	-0.2586	-0.021	0.13	0.81	0.47	5
6	0.1371	-0.1559	0.4918	-0.68	0.73	0.80	8
7	0.0982	-0.0573	1.0744	-0.65	0.88	0.66	9

A 3D plot was generated with the size of the scan on the scan point cloud on the x axis, the size of the model point cloud on the y axis and the optimal K value computed on the z axis. A best fit plane was then fitted to this plot. The equation of this best fit plane provides a mathematical solution to find the optimal K value based on the size of both the scan and model point clouds. Equation 6 shows the parametric form of the equation used to fit the plane. Table 4 shows the inputs and predictions that the model used to generate the variables.

[6] $\mathrm{K_{optimal}} = \mathrm{a_1 M} + \mathrm{a_2 S} + \mathrm{a_0}$

M and S denote to the number of points in the scene and model point clouds, respectively. a_1, a_2 and a_3 are the coefficients that were determined. MATLAB's curve fitting tool was used to best fit the plane. Table 3 summarizes the parameters calculated within their 95% confidence interval. Table 4 shows both the observed and predicted optimal K values, along with the R^2 for plane that was fit.

Table 3. Coefficients calculated for the best fit plane.

	a_0	a_1	a_2
Most Probable Value	9.14	2.706	2.05
Lower Bound Value Within %95 Level of Confidence	5.26	-1.52	-2.18
Upper Bound Value Within %95 Level of Confidence	13.02	6.93	6.27

To calculate the coefficients the input data had to be normalized. The mean and standard deviation for the number of points in the scan were calculated to be 9.3+e4 and 3.67+e4 respectively. The number of points in the model point clouds was also standardized with a mean value of 1.05+e4 and a standard deviation of 1.533+e3. Figure 7 show a graphical representation of the plane fitted to the data and the residual values between the data sets and the predictive model.

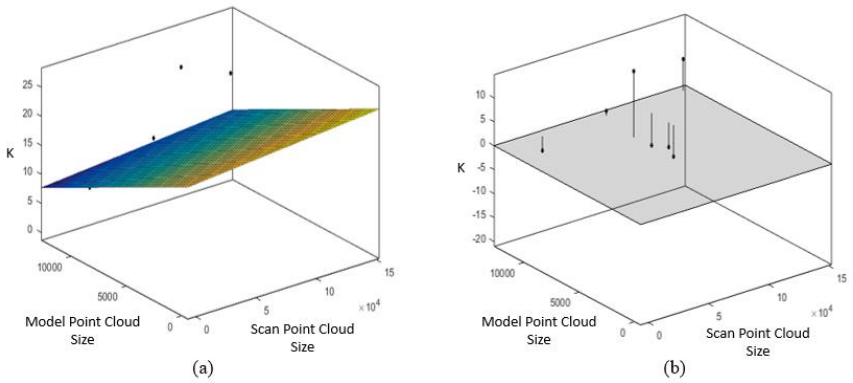

Figure 7. Graphical representation of the fitted plane to predict optimal K value. (a) 3D representation of the predictive model. (b) Residual values from the predictive plane.

To determine the goodness of fit, R^2 was calculated. R^2 was calculated by dividing the sum of squares due to regression (SSR) over total some of squares (SST).

Table 4. Comparison of the calculated K values and the predicted values using the fitted plane along with a measure of the goodness of fit.

	Observation		Predicted	SSE	SST	SSR	R^2
Scene Size	Model Size	Optimal K	Optimal K				0.75
81272	12061	11	10	1	3.45	0.73	
145265	12061	14	11	49	78.45	3.45	
28009	12061	6	9	9	9.87	0.02	
108007	8864	7	14	49	4.5	23.59	
108007	10841	5	12	49	17.16	8.16	
108007	9327	8	13	25	1.306	14.87	
74569	8864	9	15	36	0.02	34.30	
	Mean	8.6	Sum	218	114.85	1 880	

5 Conclusions and Future Work

This paper presented a case study in which clutter points were optimally removed from a scan point cloud. A mathematical closed form solution was provided for calculating the optimal K value for removing clutter points in a point cloud based on number of points in scan and model point clouds using a KNN algorithm. Experimental data was gathered by scanning a pipe spool assembly under different configurations with respect to the compliance of the assembly. The individual spools from the assembly were also experimented on individually to provide additional data points to develop a more accurate model. A plane was ultimately fitted to the data providing an R square value of 0.75.
To develop a more widely adaptable model, objects with different geometric shapes have to be tested using the developed algorithm.

While KNN is a simple, robust and effective method for classification of points as being either part of the object of interest or as clutter, it is ineffective when it is assessing a scan of an object that has a gross misalignment compared to its model. With respect to pipe spools, two examples of gross misalignment that make KNN ineffective are: when a pipe that is substantially longer than the design is used and when an elbow is installed with a 90º rotation from the design. In both of these instances, KNN will not recognize the points in the scan that do not correspond to the model are part of the erroneous assembly and will remove these points as if they are clutter.

The authors will pursue more accurate prediction models such as, neural networks, Bayesian network and other machine learning algorithms to develop a more robust solution for clutter removal. However, depending on the application, mathematical closed form models may not be accurate enough and are vulnerable to errors.

Acknowledgements

The authors would like to thank Stacey Jenson Rose and Scott Waters from Aecon, Canada, for their invaluable insights and feedback on this work. This research is partially funded by Natural Science and Engineering Research Council (NSERC) Canada and Aecon Industrial West (AIW), Edmonton, Canada.

References

Akinci, B., Boukamp, F., Gordon, C., Huber, D., Lyons, C., & Park, K. 2006. A formalism for utilization of sensor systems and integrated project models for active construction quality control. *Automation in Construction*, **15**(2): 124–138.

Amann, M.C., Bosch, T., Lescure, M., Myllyla, R. and Rioux, M. 2001. Laser ranging: a critical review of usual techniques for distance measurement. *Optical engineering,* **40**(1): 10-19.

Bosche, F. & Haas, C.T., 2008. Automated retrieval of 3D CAD model objects in construction range images. *Automation in Construction*, **17**(4): 499–512.

Brilakis, I., Dai, F. & Radopoulou, S.-C., 2012. Achievements and Challenges in Recognizing and Reconstructing Civil Infrastructure. *15th international conference on Theoretical Foundations of Computer Vision: outdoor and large-scale real-world scene analysis*. Springer-Verlag, pp. 151–176.

Burati Jr, James L., Jodi J. Farrington, and William B. Ledbetter. Causes of quality deviations in design and construction. *Journal of construction engineering and management* **118**(1): 34-49.

Corsini M, Cignoni P, Scopigno R. 2012. Efficient and flexible sampling with blue noise properties of triangular meshes. *IEEE Transactions on Visualization and Computer Graphics*,**18**(6): 914-24.

Czerniawski, T., Nahangi, M., Walbridge, S., & Haas, C. 2016. Automated Removal of Planar Clutter from 3D Point Clouds for Improving Industrial Object Recognition. *ISARC. International Symposium on Automation and Robotics in Construction.* **33**: 1

Friedman, Jerome H., Jon Louis Bentley, and Raphael Ari Finkel. 1977. An algorithm for finding best matches in logarithmic expected time. *ACM Transactions on Mathematical Software (TOMS)* **3**(3): 209-226.

Furht, B. and Ahson, S.A. eds. 2008. *Handbook of mobile broadcasting: DVB-H, DMB, ISDB-T, and mediaflo*, CRC Press.

Golparvar-Fard, M. et al. 2009. Visualization of Construction Progress Monitoring with 4D Simulation Model Overlaid on Time-Lapsed Photographs. *Journal of Computing in Civil Engineering*, **23**(6): 391–404.

Guo, G., Wang, H., Bell, D., Bi, Y. and Greer, K. 2003. KNN model-based approach in classification. *OTM Confederated International Conferences" On the Move to Meaningful Internet Systems"*, pp. 986-996.

Jiang, L. et al., 2007. Survey of Improving K-Nearest-Neighbor for Classification. *Fourth International Conference on Fuzzy Systems and Knowledge Discovery,* pp. 679–683.

Kohavi, Ron. 1996. Scaling Up the Accuracy of Naive-Bayes Classifiers: A Decision-Tree Hybrid. *KDD*, **96**: 202-207.

Lee, J. et al., 2012. Automated pipeline extraction for modeling from laserscanned data.

Lee, J., Kim, C., Son, H. and Kim, C.H. 2012. Automated pipeline extraction for modeling from laser scanned data. *International Symposium on Automation and Robotics in Construction (ISARC)*.

Liu, T., Moore, A.W. & Gray, A. 2006. New Algorithms for Efficient High-Dimensional Nonparametric Classification. *Journal of Machine Learning Research*, pp.1135–1158.

Nahangi, M. et al. 2015. Automated assembly discrepancy feedback using 3D imaging and forward kinematics. *Automation in Construction*, **56**: 36–46.

Nahangi, M., Czerniawski, T., Haas, C.T., Walbridge, S. and West, J. 2015. Parallel systems and structural frames realignment planning and actuation strategy. *Journal of Computing in Civil Engineering*, **30**(4): 04015067.

Pan, R. & Taubin, G. 2016. Automatic segmentation of point clouds from multi-view reconstruction using graph-cut. *The Visual Computer*, **32**(5), pp.601–609..

Papazov, C. and Burschka, D. 2010. An efficient ransac for 3d object recognition in noisy and occluded scenes. *Asian Conference on Computer Vision,* pp. 135-148.

Remondino, F. et al. 2015. Image-based 3D modeling of the Erechteion, Acropolis of Athens. vol. 37 of The international archives of the photogrammetry, remote sensing and spatial information sciences, ISPRS, pp. 1083–1091

Sharif, M.-M. et al. 2016. A Preliminary Investigation Of The Applicability Of Portable Sensors For Fabrication And Installation Control Of Industrial Assemblies. *Canadian Society for Civil Engineering*. London, ON, Canada.

Xie, Z. et al. 2002. SNNB: A Selective Neighborhood Based Naïve Bayes for Lazy Learning. *Pacific-Asia Conference on Knowledge Discovery and Data Mining*, pp. 104–114.

Zhao, C. & Meng, X. 2009. An Improved Algorithm for k-Nearest-Neighbor Finding and Surface Normals Estimation. *Tsinghua Science & Technology*, **14**: 77–81.